PERGAMON

Journal of Structural Geology 24 (2002) 1125–1137

JOURNAL OF STRUCTURAL GEOLOGY

www.elsevier.com/locate/jstrugeo

The equilibration of high-angle grain boundaries in dynamically recrystallized quartz: the effect of crystallography and temperature

Jörn H. Kruhl*, Mark Peternell

Technische Universität München, Faculty of Civil and Geodetic Engineering, Section Tectonics and Material Fabrics/Chair of General, Applied and Engineering Geology, D-80290 München, Germany

Received 21 February 2001; revised 1 June 2001; accepted 6 June 2001

Abstract

Dynamically recrystallized and sutured quartz grains from metamorphic rocks with different strain intensities and temperature conditions ranging from ca. 350°C to ca. 700°C have been studied. Universal-stage measurements on quartz–quartz high-angle grain boundaries show that they are never curved but always consist of straight segments which preferentially occupy specific crystallographic orientations in relation to both neighboring crystals. With increasing temperature the segments preferentially concentrate in a decreasing number of orientations, mainly near the rhombohedral $\{10\bar{1}1\}$ planes. The crystallographic data and the observations on grain boundary geometries suggest that: (i) grain boundary orientations are strongly crystallographically controlled, (ii) this control is the main factor on the textural equilibration of quartz–quartz grain boundaries in metamorphic rocks, and (iii) grain boundaries from dynamically recrystallized quartz should be regarded as annealed and equilibrated fabrics that are stable against subsequent annealing as long as the material is not re-deformed.

Keywords: Recrystallized quartz; Crystallographic orientation; High-angle grain boundaries; Textural equilibrium

1. Introduction

Properties of crystalline materials are highly dependent on the nature of the boundaries between crystals of different or the same minerals. These interphase or grain boundaries influence the strength of the material as well as fluid-permeability and, consequently, reactivity and susceptibility to weathering. Grain boundaries, i.e. boundaries between crystals of the same material and crystal structure but different orientation, are formed and changed by deformation and heating and, therefore, provide information about the material history. The principal process of formation and variation of grain boundaries is recrystallization, defined as "formation and migration of high-angle boundaries" (Vernon, 1976, p. 166) or as "deformation-induced reorganization of grain size, shape and/or orientation with little or no chemical change" (Poirier and Guillopé, 1979). Following Voll (1969), we distinguish between two different types of recrystallization: 'dynamic' if differential stress is present and 'static' if it is absent. During dynamic recrystallization, either by subgrain rotation or grain boundary bulging (Passchier and Trouw, 1996), the new grains are immediately deformed and themselves involved in the recrystallization process. Moreover, if strain-induced migration of grain boundaries is present, neighbouring grains may increasingly interfinger. In general, a dynamic balance is reached between the formation (and growth) of new grains and the restructuring of already deformed grains.

Grain boundary migration during dynamic recrystallization may lead to intense grain boundary suturing due to differences in lattice defect densities in neighbouring crystals (Fig. 1A–D). That part of a crystal with relatively lower defect density grows into that part of the neighbouring crystal with relatively higher defect density. The regions behind a migrating boundary are strain free and show a considerable decrease in the number of lattice defects. Grain boundary patterns, i.e. the geometry of grain boundaries and grain boundary networks, are dependent on several factors, most important among them temperature/strain rate, strain and differential stress. Moderate deformation at lower greenschist facies conditions may lead to incomplete recrystallization with old grains surrounded by new and smaller ones (Fig. 1A). With increasing temperatures, on a statistical basis, grain boundary sutures become coarser (Fig. 1C), whereas an elevated differential stress reduces the sizes of the recrystallized grains as well as of the grain boundary sutures (Fig. 1D).

With respect to quartz, Voll (1969, p. 117) pointed to the

* Corresponding author. Fax: +49-89-2892-5852.
E-mail address: joern.kruhl@geo.tum.de (J.H. Kruhl).

0191-8141/02/$ - see front matter
PII: S0191-8141(01)00096-7

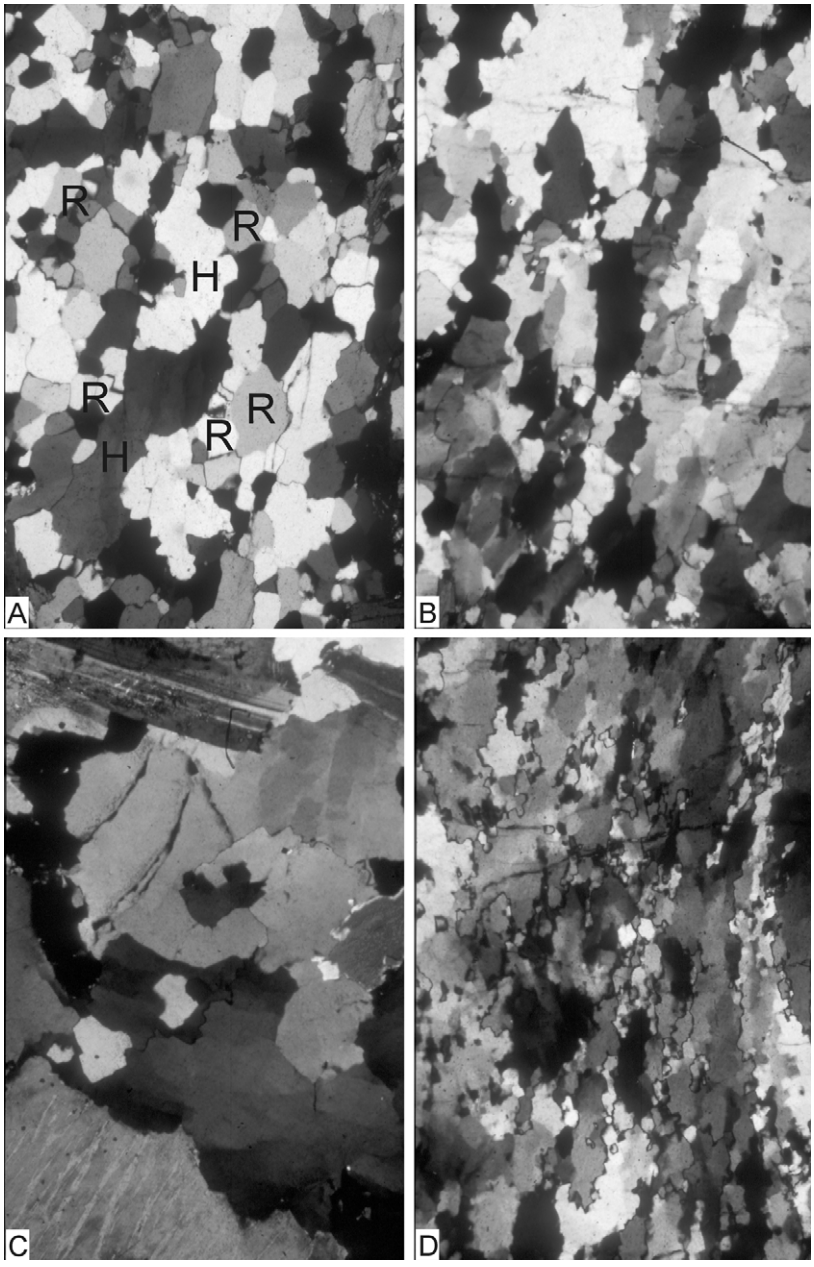

Fig. 1. Microphotographs of the analyzed thin sections; crossed polarizors. (A) Sutured grain boundaries in recrystallized igneous quartz grains from a late-Hercynian granite of the Aar Massif (Central Swiss Alps), with relics of host grains (H) and with smaller recrystallized grains (R), deformed under lower greenschist facies conditions during the Alpine orogeny (Lepontine event) (Trümpy, 1980); near Erstfeld, south of Lake Lucerne (Switzerland); sample KRA3; long side of microphotograph (LS) = 3.1 mm. (B) Coarsely sutured quartz grain boundaries from an orthogneiss of the Monte Rosa Nappe, deformed under lower amphibolite facies conditions (Kruhl, 1979) during the Alpine orogeny (Lepontine event); south of Malesco (Val Viggezzo, Northern Italy); sample KR705; LS = 3.1 mm. (C) Coarsely sutured quartz grain boundaries from a syntectonic granite (Fichtelgebirge, Saxothuringian Zone, Central European Variscides; Hecht et al., 1997); sample LHG4; LS = 3.1 mm. (D) Sutured grain boundaries from recrystallized quartz grains of a lower amphibolite facies shear zone (Altenberger and Kruhl, 2000) of the fossil Hercynian lower crust of Calabria (Southern Italy); sample KR3263; LS = 1 mm.

fact that, for deformation and strain-induced grain boundary migration, increasing temperature causes grain boundary segments to increase in size and also to become preferentially oriented parallel to rhombohedral planes. The increase of segment length with temperature is also reflected by an increasing ratio of the number of long versus the number of short segments, which leads to a decreasing fractal dimension of the grain boundary pattern (Kruhl and Nega, 1996). The development of preferred crystallographic orientations has also been shown for quartz boundaries in quartz foam textures (Kruhl, 2001). However, such crystallographic control of grain boundaries needs further attention since it may provide information about: (i) the nature of grain boundaries, (ii) the process of restructuring of grain boundary patterns, and (iii) the influence of physical conditions, mainly that of temperature.

The present study concentrates on sutured grain boundaries in quartz deformed under conditions of lower greenschist and lower amphibolite facies, and in quartz from a syntectonic granite. As microtextures in all investigated samples show, at least during the late stage of deformation, grain boundary migration was the dominant recrystallization process. Data on the preferred crystallographic orientation of grain boundary segments and their variation with different temperatures are presented. Based on these data, the process of grain boundary migration and 'stabilization', and the consequences for the development of grain boundary patterns, will be discussed.

2. Measurements

2.1. Instrument and method

Grain boundary patterns of transparent crystalline material are typically studied in thin sections under the polarizing microscope. In this way the pattern can be recorded in two dimensions or in a ca. 30 μm thick layer, respectively. In addition, the universal stage (henceforth u-stage; von Federow, 1893; Sarantschina, 1963; and others) serves as the only instrument to measure the spatial orientation of small grain boundary areas (segments) with sufficient accuracy and in large number. These segments are brought to a position perpendicular to the microscope stage, i.e. into parallelism to the direction of view. Thus, even micrometer-scale details of the grain boundary geometry are revealed which, due to the reflection of the light beam, would otherwise remain undetected even with only slight inclination of the boundaries against the vertical. After a generally straight segment (see further below) has been brought to a position parallel to the N–S direction of the ocular cross wires, its orientation is measured. The optical axis of the quartz (the *c*-axis) is measured in horizontal E–W or in vertical orientation. The advantage of the combined information about *c*-axis and grain boundary orientation warrants the high expenditure of time that can be reduced by the use of a digitizing u-stage. In quartz, as in any other optically uni-axial mineral, no other crystallographic direction can be measured than the *c*-axis. Consequently, only the angle between the *c*-axis and the grain boundary pole can be determined and it is not possible to determine unequivocally the crystallographic orientation of any grain boundary segment. However, in the trigonal system specific sets of crystallographic planes, different only in sign, exhibit the same characteristic angle to the *c*-axis. Therefore, it is justified to correlate specific angles with specific sets of crystallographic planes, because tests have shown that in the studied samples grain boundary segments around one single quartz grain are grouped in specific orientation maxima that can be related to specific low-index planes. In addition, the conclusions of the present study are mainly related to general aspects of the crystallographic control during grain boundary development and not to specific planes of different sign or only slightly different orientation.

We have measured: (i) the orientation of straight grain boundary segments, (ii) their lengths, and (iii) the *c*-axis orientations of the two neighboring quartz grains or subgrains, respectively. The accuracy of measurement has been estimated on the basis of repeated measurements. The directions (azimuth) of grain boundary poles and *c*-axes vary up to 1°, and their dip-angles up to 2°. Outliers of up to 4° may occur if the dip-angles are higher. The variation of the angle between a grain boundary pole and a *c*-axis is as high as 2.5°, with outliers of up to 4°. The accuracies of the grain boundary and *c*-axis measurements are equal. However, the directions (azimuth) of grain boundary poles and *c*-axes can be measured with more precision than their dip angles. High dip-angles are the least accurate. Consequently, the orientation of flat-lying *c*-axes or steep grain boundary segments can be more precisely determined than more strongly inclined *c*-axes or gently dipping boundary segments. In addition, there is a cut-off effect on the u-stage measurements. Since the u-stage can be inclined only up to ca. 50° as a maximum, grain boundary segments that are inclined less than 40° to the microscope stage cannot be measured. For example, if the *c*-axis is perpendicular to the thin-section plane, grain boundary segments perpendicular or sub-perpendicular to the *c*-axis, i.e. the basal plane or specific rhombohedral planes, cannot be measured. If the *c*-axis is parallel to the thin-section the basal plane can be measured; however, specific rhombohedral and prismatic planes cannot be measured. Consequently, the probabilities of specific angles between the boundary segment poles and the *c*-axis are changed. In general, the effect of the limited u-stage inclination on the frequency distribution of these angles can be avoided by measuring quartz grains with a broad variation of *c*-axis orientations, as has been done for the present study. It should be noted that this orientation has to be nearly random only in relation to the dip-angle of the *c*-axes against the thin-section plane but not in relation to the 3D distribution of the axes. A correction of the uniform distribution is only necessary for a strong preferred orientation of quartz *c*-axes dip-angles, e.g. if quartz [*c*] clusters around one specific direction. Only slightly non-random dip-angle distributions, as those of the presented *c*-axis orientations, do not noticeably affect the uniform distribution because of the 50°-rotation possibility of the u-stage, by which an uneven probability of grain boundary orientations is strongly smoothed.

The combination of u-stage based grain boundary orientation measurements with modern electron backscatter diffraction (EBSD) techniques (Lloyd, 1987; Kunze et al., 1993; Prior et al., 1996) would provide more complete information about the crystallographic orientation of the quartz grain boundaries. However, it will be shown in this paper that the combination of the grain boundary orientation with merely the *c*-axis provides useful information. Nevertheless, our study should be regarded as a preliminary one, which gives basic

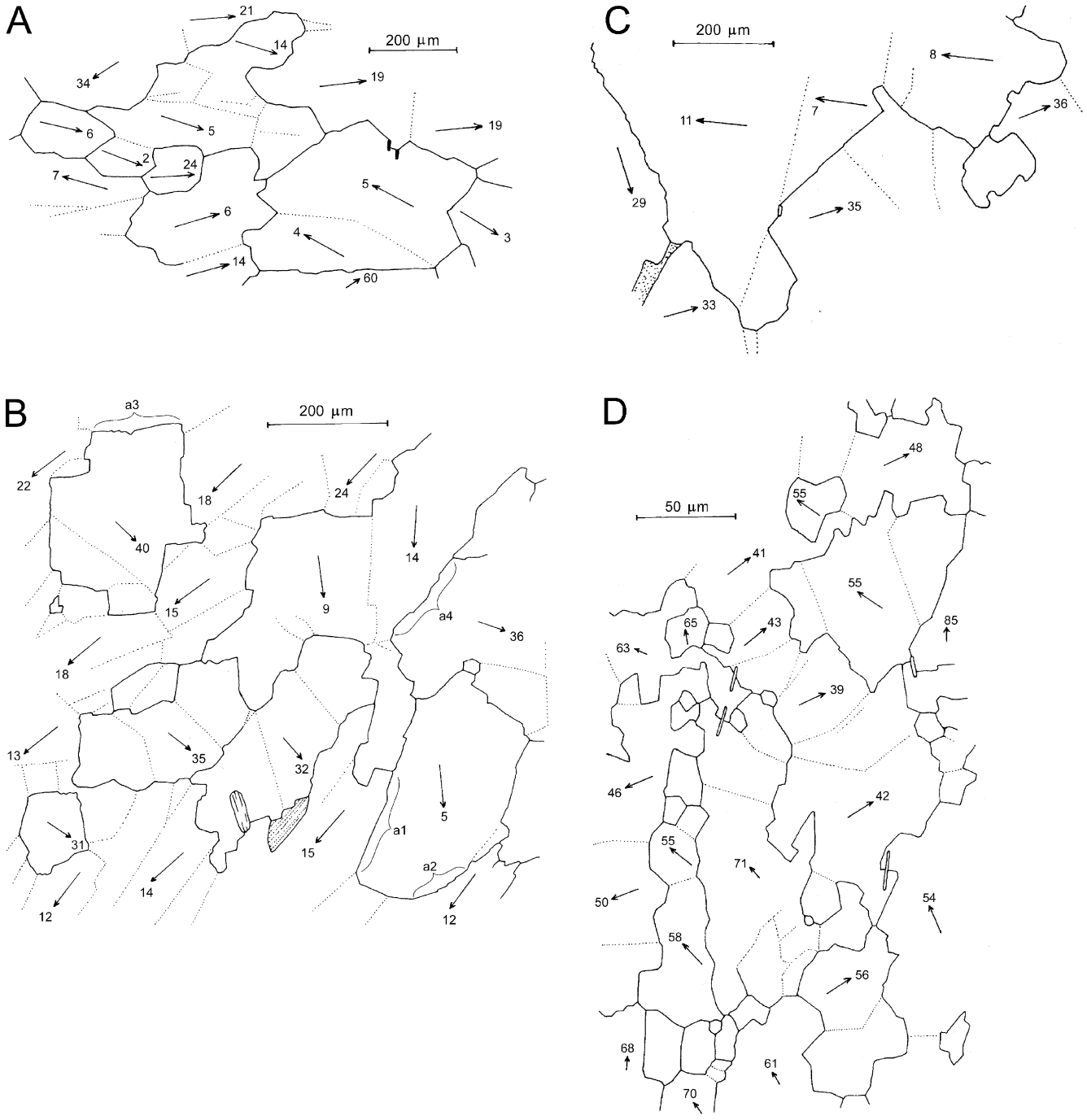

Fig. 2. Thin section sketches of the measured sutured quartz grain boundary patterns. All boundary segments are figured in a position perpendicular to the thin-section plane (by universal-stage rotation). Locally, steps of relatively short segments interrupt relatively long segments of similar orientation as indicated in (B) (a1–a4). Solid lines = high-angle boundaries; stippled lines = low-angle (subgrain) boundaries. The dip-directions (arrows) and dip-angles of representative quartz *c*-axes are indicated. (A) Sample KRA3; (B) sample KR705; (C) sample LHG4; (D) sample KR3263.

data and suggestions for future work, which should include EBSD and other SEM and TEM techniques.

2.2. The samples and their deformation and metamorphism conditions

Quartz crystals from four different rocks — two orthogneisses, one syntectonic granite and one mylonite from a leucosome layer — have been studied. The rocks experienced different temperatures and strain. All measurements were made on pure quartz grain aggregates that represent former igneous crystals. Three of the four studied samples (A,B,C) are from 'normal' regional-metamorphic rocks, which we assume experienced 'normal' strain rates. One

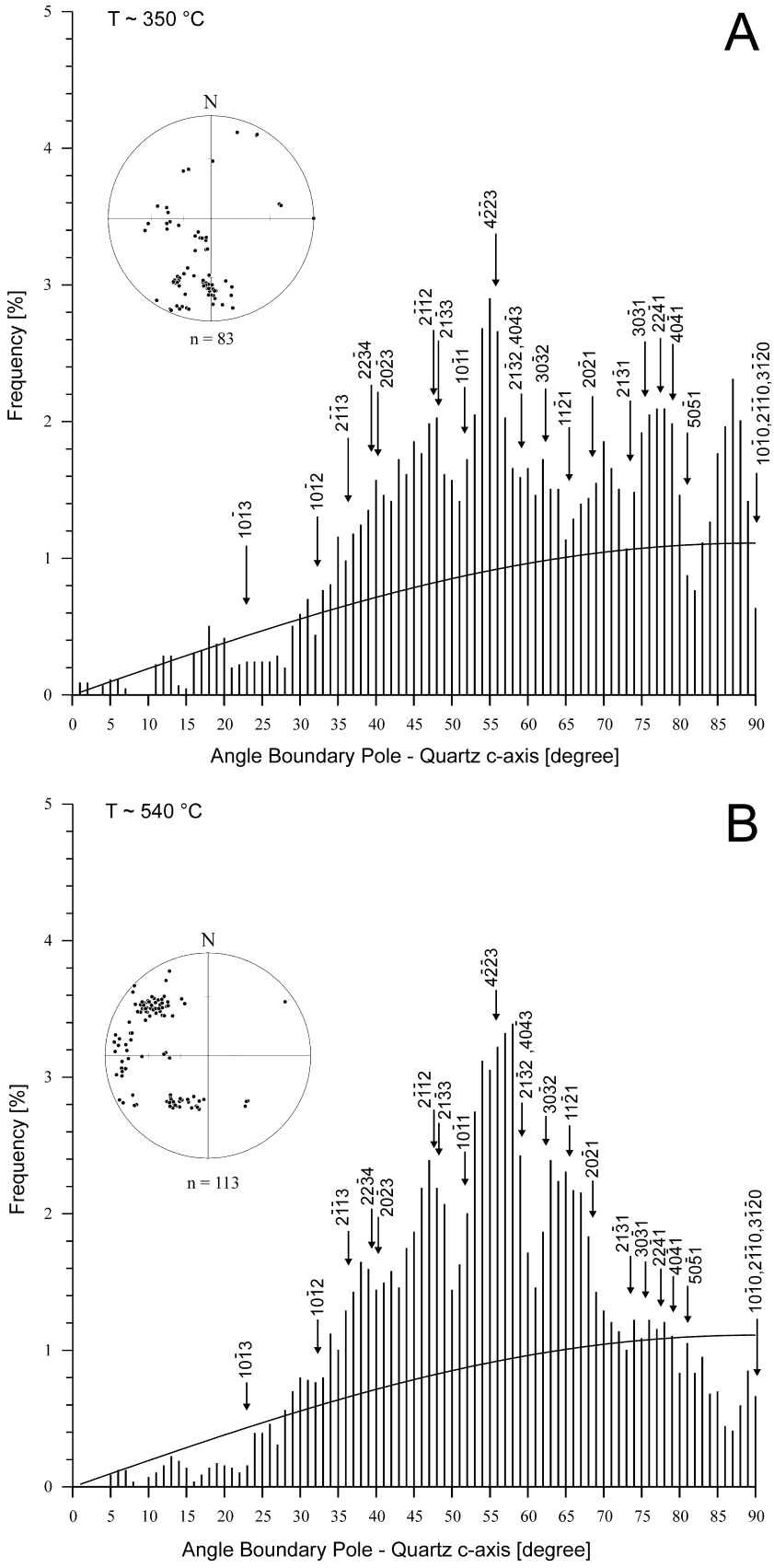
T ~ 350 °C
A
N
n = 83
Frequency [%]
Angle Boundary Pole - Quartz c-axis [degree]
T ~ 540 °C
B
N
n = 113
Frequency [%]
Angle Boundary Pole - Quartz c-axis [degree]

Fig. 3.

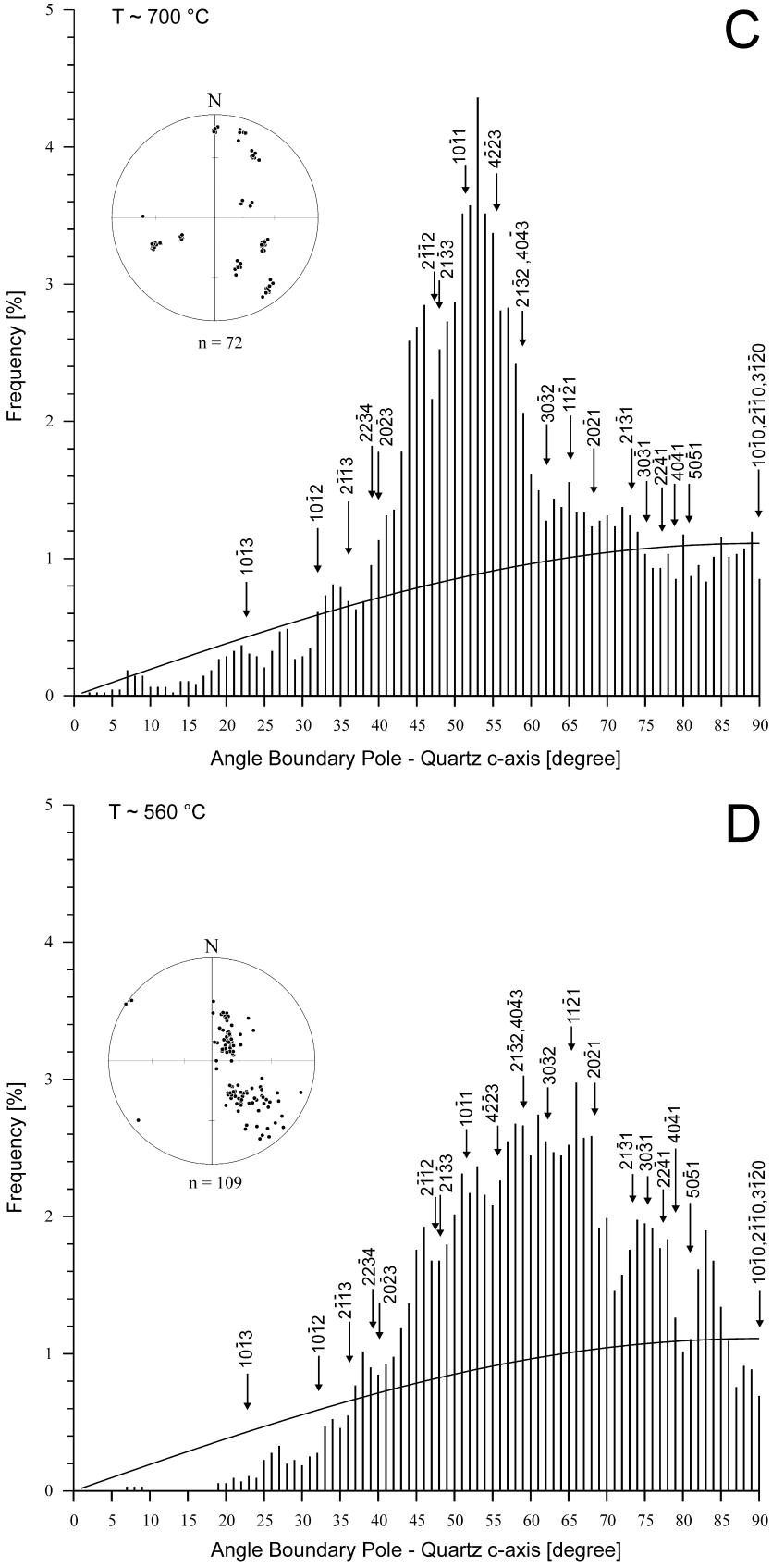

Fig. 3. (*continued*)

sample (D) is a mylonite, presumably with increased flow stress and strain rate. During deformation and afterwards, in the samples A, B and D quartz occurred naturally as low-quartz, and in sample C possibly as high-quartz.

(A) *Sample KRGA3* is an orthogneiss from the Aar massif (Central Switzerland, south of Erstfeld) and the most weakly deformed sample with the lowest temperature. During the Alpine orogeny the igneous quartz partly dynamically recrystallized at temperatures of ca. 350°C (Voll, 1976) and deformed with ca. 40% flattening strain. The cooling time from peak temperatures to the lower temperature limit of quartz recrystallization (ca. 300°C; Voll, 1976) was about 3 m.y. (Wagner et al., 1977). Typically, recrystallized grains of variable size (ca. 100–500 μm) are formed around relics of host grains (Fig. 2A). Both grain types exhibit sutured grain boundaries and subgrain structures with low-angle boundaries mainly parallel to prismatic or rhombohedral planes.

(B) *Sample KR705* is an orthogneiss from the north-eastern Sesia Zone (Western Alps), which was deformed (approximately 60% flattening strain) during increasing temperatures up to ca. 540°C (Kruhl, 1979). The cooling time from these peak temperatures to ca. 300°C is estimated as nearly 10 m.y., based on cooling ages from the nearby Simplon–Antigorio region (Wagner et al., 1977). The dynamically recrystallized quartz forms strongly sutured grains with predominantly prismatic subgrain boundaries (Fig. 2B). In comparison with sample KRGA3 the recrystallized grains are larger, although this is partly concealed by the higher degree of suturing.

(C) *Sample LHG4* has been taken from a late-Variscan granite of the Fichtelgebirge (Saxothuringian Zone, Central-European Variscides). The crystallization and, therefore, deformation temperatures have been estimated at ca. 700°C (Hecht et al., 1997). K/Ar biotite and white mica ages indicate cooling of the granite within a few million years as a maximum (Siebel et al., 1997). The granite was weakly deformed during crystallization. Consequently, the igneous quartz grains are still visible but show coarse grain boundary suturing and a weak polygonization with prismatic and rhombohedral but also frequently basal subgrain boundaries (Fig. 2C). The straight suture segments are up to ca. 150 μm long, but may also be as short as only a few micrometers.

(D) *Sample KR3263* is a 'dry' mylonite of the fossil Variscan lower crust of Calabria (S. Italy). Mylonitization occurred at ca. 560°C (Altenberger and Kruhl, 2000). Cooling to ca. 300°C lasted approximately 110 m.y. (Schenk, 1989; Altenberger and Kruhl, 2000). Mylonitization led to dynamic recrystallization of quartz with variable grain sizes ranging from only a few micrometers to more than 100 μm (Fig. 2D). The coarser grains are strongly sutured and polygonized, with prismatic and rhombohedral subgrain boundaries. On average, the straight segments of the sutures are clearly shorter than those in the other samples, from ca. 20 μm down to the magnification limits of the microscope of about 1 μm.

Transitions from subgrains to recrystallized grains were not observed in any of the samples. Therefore, at least during the last stage of deformation, grain boundary migration rather than subgrain rotation was the dominant recrystallization process. After deformation all samples were annealed above the recrystallization temperature of quartz during periods from a few to more than 100 m.y. No low-temperature deformation fabrics (kinks, deformation lamellae, wavy extinction) are present.

3. The geometry and preferred crystallographic orientation of grain boundary segments

In all samples the quartz grains are more or less strongly sutured and polygonized. The grain boundary sutures are composed of straight segments with variable lengths. Grain boundary curvatures only are apparent, being due to cut-effect. If boundaries are not exactly perpendicular to the thin-section plane they appear broad, diffuse and curved under the microscope even if in reality they consist of a few straight segments of only slightly different orientation (weak curvature), or of numerous short straight segments of larger misorientation (strong curvature). Without the u-stage such a grain boundary geometry is generally undetectable.

At higher temperatures the length of individual grain boundary segments is generally increased (Fig. 2A–C). However, the quartz from the mylonite shows a decreased segment length (Fig. 2D), in accordance with the general decrease of grain size in mylonites due to a high differential stress (Passchier and Trouw, 1996). The angles between neighboring segments may vary between nearly 180° and less than 90°. Angles much below 90° are rare. Relatively long segments of similar orientation may be interrupted by steps of relatively short segments (e.g. Fig. 2B, a1–a4).

Fig. 4 shows the frequency distribution of the angles between the grain boundary segments and the *c*-axes of the two neighboring quartz grains. This represents a 'one-dimensional' distribution (henceforth: 1D distribution),

Fig. 3. Crystallographic orientation of grain boundary segments from dynamically recrystallized quartz; angle between the grain boundary pole and the *c*-axes of the two neighboring quartz grains versus frequency (percentage of total number of measurements — weight factors included); kriging over 3°. Principal crystallographic planes of quartz, the uniform distribution of any crystallographic position (solid line), and the quartz [*c*] orientations (equal angle projection — Wulff net, lower hemisphere; with the long side of the thin section as N direction) with the number of measurements are indicated. The uniform distribution is defined as 1.1111 times the sine of the angle between the grain boundary pole and quartz [*c*]. The sine defines the reduction of a 3D to a 2D uniform distribution of any direction. The factor 1.1111 is a best-fit value determined on the basis of the different maxima of the frequency distribution. The relative length of each boundary segment is used as a weight factor of the frequency. The approximate deformation temperature *T* is given for each sample. (A) Sample KRGA3; 530 measurements. (B) Sample KR705; 770 measurements. (C) Sample LHG4; 624 measurements. (D) Sample KR3263; 772 measurements.

which does not account for the fact that each grain boundary segment is related to two neighboring crystals with different orientation and different angles to the segment. The frequency distributions of the four samples clearly differ from a uniform distribution and from one another. Because the *c*-axis dip-angles of the measured quartz grains against the thin-section plane are only slightly non-random, a correction of the uniform distribution of the angles is not necessary. In comparison with the non-weighted frequency distributions (not shown here), the distributions weighted by the segment length more clearly exhibit the deviation from the uniform distribution. Consequently, the relatively long segments bear most of the crystallographic preferred orientations. The segments preferentially form angles of ca. 35–85° with the *c*-axis. Single maxima may occur within this range of preferred orientations. The most prominent ones reach values of 3–4.5%. Since the measurement inaccuracy is generally not larger than 2° we regard the positions of the maxima as significant; we do not regard the different positions of maxima in different diagrams as an effect of measurement inaccuracy. Despite similarities there are clear differences between the four diagrams.

Sample KRGA3: The most weakly deformed rock with the lowest temperature (lowermost greenschist facies) is the only one with a preferred orientation of grain boundary segments near the prism planes (Fig. 3A). Additional maxima are oriented near to 75–79°, 69–72°, 53–57° (the highest maximum), 47–48° and 39–41°, which are near the crystallographic planes $\{22\bar{4}1\}/\{40\bar{4}1\}$; $\{20\bar{2}1\}$, $\{4\bar{2}\bar{2}3\}$, $\{2\bar{1}\bar{1}2\}/\{21\bar{3}3\}$ and $\{22\bar{3}4\}/\{20\bar{2}3\}$. Those planes with angles between their poles and quartz [*c*] of less than 30° are clearly less represented.

Sample KR705: The grain boundary segments from lower amphibolite facies conditions show a reduced range of crystallographic preferred orientations (Fig. 3B). Maxima occur between ca. 35 and 70°. This concentration of preferred orientation goes along with an enlargement of the maxima. The highest maximum at 53–59° reaches nearly 3.4%. The next highest maxima are oriented at 62–68° and 45–49°. There is no pronounced maximum near the prism planes. The low frequency of prism planes is most probably caused by the absence of *c*-axes with dip angles larger than ca. 45° against the thin-section plane.

Sample LHG4: The range of preferred crystallographic orientation is even more reduced in quartz from the syntectonic granite. There is only one broad prominent maximum between ca. 43 and 60°, with the peak of nearly 4.4%, the highest peak in the four diagrams, at 53°, which is near to the $\{10\bar{1}1\}$ plane (Fig. 3C).

Sample KR3263: The lower amphibolite facies mylonite shows a broad preferred orientation of angles between ca. 43 and 85° with only weak single maxima (Fig. 3D). The highest maximum reaches 3%. Planes parallel to or near the basal plane are statistically less represented.

In order to obtain information about the relationship between the two neighboring crystals and the grain boundary segments in between, the frequency distribution of the two connected angles has to be considered. For that purpose the angle between the grain boundary pole and quartz [*c*] of one neighboring crystal has been plotted versus the angle between the grain boundary pole and quartz [*c*] of the other neighboring crystal (Fig. 4). This 'two-dimensional' distribution (henceforth: 2D distribution) reveals further information. There is the same general tendency of concentration of the frequency distribution with increasing temperatures, however, with a much stronger dispersion into single maxima.

Sample KRGA3 (Fig. 4A): The frequency distribution is comparatively weak and subdivided into several mostly weak maxima, which do not always occur at angles forming maxima in the 1D distribution (Fig. 3A). For example, maxima are located at angles of ca. 50°/42° and 60°/60°, although these angles do not form prominent maxima in the 1D distribution. Strong maxima of the 1D distribution are dispersed in the 2D distribution into several partly weaker maxima (e.g. maxima at 85–89° or at 75–79° in Fig. 3A), whereas the maxima at 69–72° and 85–89° are equivalent to only one strong maximum in the 2D distribution. On the other hand, the combination of two maxima from the 1D distribution does not necessarily form a maximum in the 2D distribution. For example, the combination of angles in the range of 53–57° (the strongest maximum in the 1D distribution in Fig. 3A) and 69–72°, or the combination of 85–89° and 75–79°, do not form strong maxima in the 2D distribution. 'Twin positions' (combinations of two angles of the same or similar size), which plot along the hypotenuse of the triangle, preferentially occur between ca. 45 and 65° with the strongest maximum at $\{2\bar{1}\bar{1}2\}$ (the Japanese twin position), and a second maximum about $\{21\bar{3}2\}/\{40\bar{4}3\}$.

Sample KR705 (Fig. 4B): In the 2D distribution a smaller area with higher maxima is developed. The principal maximum of the 1D distribution at 53–59° forms five maxima in the 2D distribution, the weakest one together with angles in the range of 85–90°, which is below the uniform distribution in Fig. 3B, and four strong ones with angles in the range of 63–68°, 56–59° (i.e. a 'twin position'), 46–48°, and 39–40°. Again, these angles represent maxima in the 1D distribution; however, their combination does not form a maximum in the 2D distribution. One stronger 'twin position' is developed about 45°, near the Japanese twin position.

Sample LHG4 (Fig. 4C): This distribution is concentrated in an even smaller area. The strong maximum at 48–57° of the 1D distribution (Fig. 3C) is related to the principal maximum at the same angles in the 2D distribution. The smaller maxima of the 2D distribution are not clearly expressed in the 1D distribution. The principal maximum of the 2D distribution is oriented close to the hypotenuse of the triangle diagram (Fig. 4C), close to the Estérel twin position at $\{10\bar{1}1\}$.

Sample KR3263 (Fig. 4D): Although the 1D distribution (Fig. 3D) is broadly dispersed in the range between 37 and

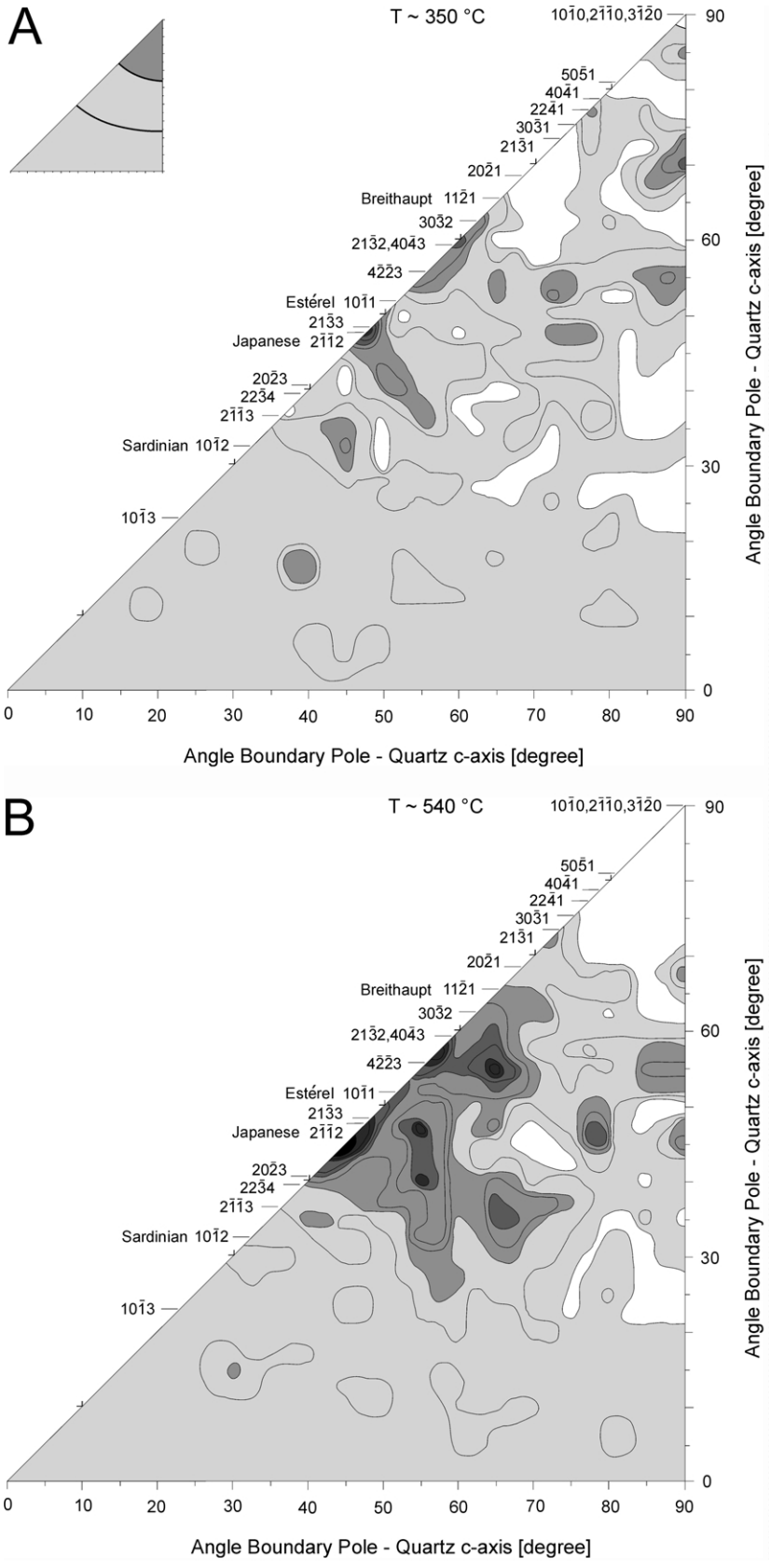
A
T ~ 350 °C
B
T ~ 540 °C
Breithaupt 11$\bar{2}$1
Estérel 10$\bar{1}$1
Japanese 2$\bar{1}\bar{1}$2
Sardinian 10$\bar{1}$2
10$\bar{1}$3
Angle Boundary Pole - Quartz c-axis [degree]
0
10
20
30
40
50
60
70
80
90

Fig. 4.

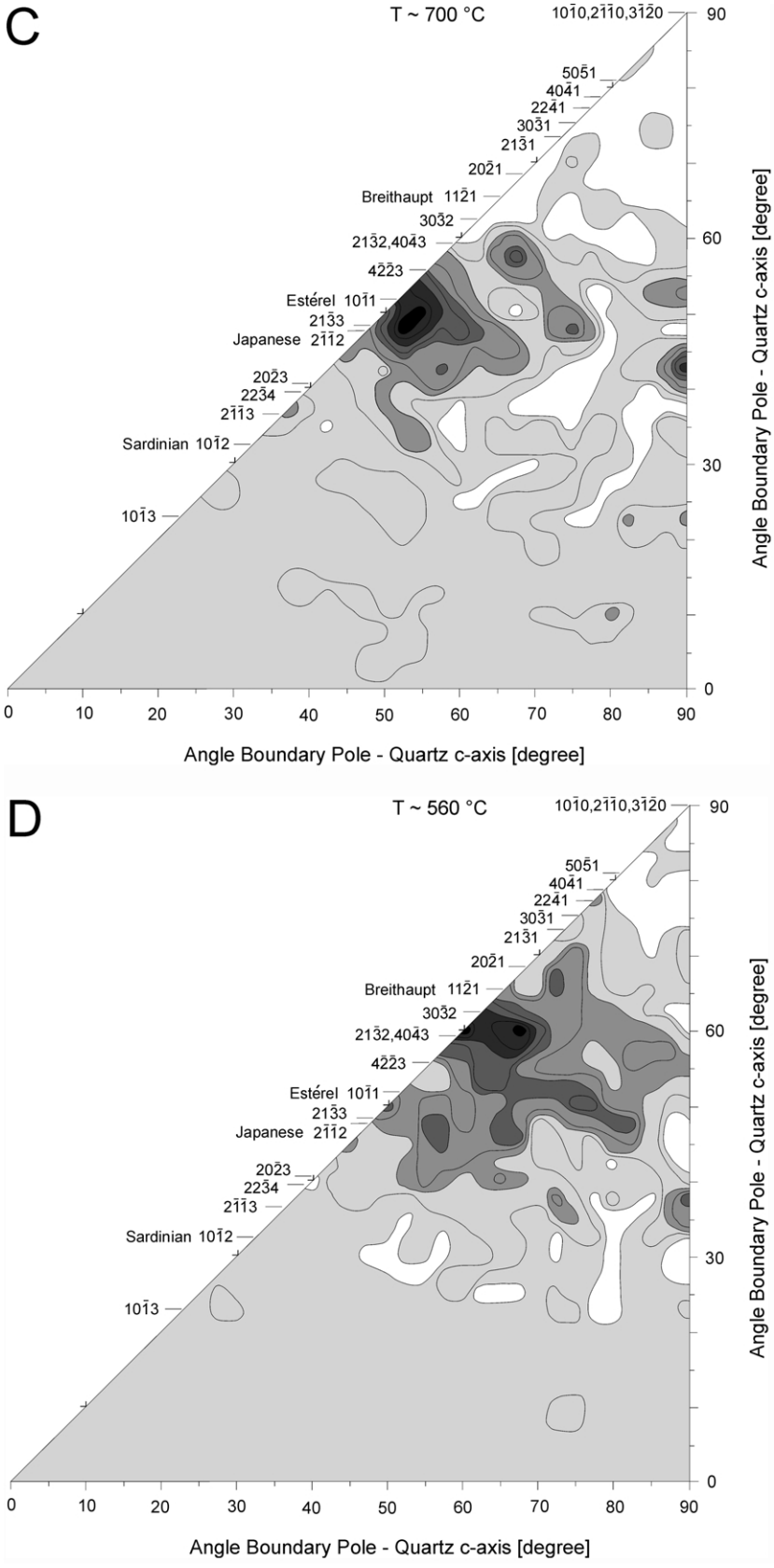

Fig. 4. (*continued*)

85° and does not exhibit many clear maxima as the 1D distributions of the other samples, the 2D distribution develops a clear maximum at 60–70° in combination with 57–62°. Additional but weaker maxima appear as combinations of angles that form only weak or no single maxima in the 1D distribution. A strong 'twin position' is developed at ca. 60°, and a weaker one at 50°.

In general, in the 1D as well as the 2D distributions, the grain boundary segments clearly prefer rhombohedral, as well as pyramidal and trapezohedral, positions compared with basal or prismatic orientations. The 2D distributions are more strongly subdivided in comparison with the 1D distributions. The maxima of the 2D distributions are formed by certain, but by no means all, angles, which form maxima in the 1D distributions. Combinations of all angles, which represent maxima in the 1D distributions, do not necessarily form maxima in the 2D distributions. 'Twin positions', or combinations of two angles of the same or similar size, are only favoured at certain angles. In general, there is a specific development of the frequency distribution patterns (Figs. 3 and 4) in relation to the temperature. With increasing temperatures, from Fig. 4A to B to C, the number of distinct maxima decreases and the grain boundary segments increasingly concentrate in the range of ca. 48–57° in relation to quartz [*c*], i.e. near the $\{10\bar{1}1\}$ rhombohedral planes. This tendency even includes the mylonite with its strong quartz deformation and recrystallization.

4. Discussion

Although there is some evidence from studies on metals and ceramics that migrating boundaries have a different structure than stationary boundaries (Kingery, 1974; Gleiter, 1982), we would like to emphasize that our investigation is related to stationary boundaries, which acquired their present status after deformation and during annealing.

On the basis of our investigation, previously presented data about the geometry and the crystallographic control of quartz grain boundaries (Voll, 1969; Kruhl, 2001) can be completed and made precise. Sutured grain boundaries from dynamically recrystallized quartz grain aggregates are never 'curved' but always consist of straight segments (Fig. 2). These segments may occupy any crystallographic orientation in relation to the neighboring quartz grains: low- to high-index or even irrational. However, there are preferred orientations mainly parallel to rhombohedral and trigonal pyramidal planes. In detail, grain boundary segments may be preferentially oriented in two different low-index positions in relation to the two neighboring quartz crystals, but also in a low-index position to one crystal and in a high-index or irrational position to the other one. These observations are valid down to the resolution limit of the microscope-u-stage system (ca. 1 μm). We do not see good arguments that numerous steps of low-index planes on the submicroscopic scale form high-index or irrational orientations, in reality. First, high-resolution TEM studies on metals and ceramics show straight grain boundary segments on the nanometer scale that also frequently occupy high-index or even irrational orientations and are only rarely decomposed to short steps of low-index planes on the atomic scale (Norton and Carter, 1992; Wolf and Merkle, 1992). Second, if grain boundaries would be generally stabilized by such small steps of low-index planes it should be expected that they form, on the microscope scale, curved boundaries of whatever shape. This is not the case.

The preferred grain boundary orientations are roughly dependent on temperature, as presented in Figs. 3 and 4. At lower greenschist facies conditions several weak maxima of different rhombohedral and pyramidal positions occur (Fig. 3A). This pattern and that of the 2D distribution (Fig. 4A) are similar to patterns that developed at similar temperatures in quartz foam textures, which are textures of static recrystallization and annealing (Kruhl, 2001, Figs. 11A and 12). Even if the significance of single maxima within such a weak frequency distribution is questionable, the pattern itself and its variation with increasing temperatures bear useful information. At lower amphibolite facies temperatures and at crystallization conditions of a syntectonic granite the grain boundary segments increasingly concentrate in the rhombohedral positions near $\{10\bar{1}1\}$ (Figs. 3B and C and 4B and C). Consequently, these positions are also favored between neighboring quartz crystals with *c*-axis orientations approximately perpendicular to each other (Fig. 2B), and an approximately rectangular grain boundary pattern is developed as is common in high-grade regional or contact metamorphic rocks (Voll, 1969, Fig. 50; Gapais and Barbarin, 1986, Fig. 4; Masberg et al., 1992, Fig. 3; Büttner and Kruhl, 1997, Fig. 6d). The crystallographic control on the orientation of straight grain boundary segments may serve as a general explanation of the development of such rectangular grain boundary

Fig. 4. Angle between the grain boundary pole and the *c*-axis of one neighboring quartz grain versus angle between the grain boundary pole and the *c*-axis of the other neighboring grain; same measurements as in Fig. 3. The number of measurements in each $2.5 \times 2.5°$ square area has been determined, with corrections along the hypotenuse of the triangle diagram where only half of a square is present. In order to smooth the frequency distribution, kriging with areas of $5 \times 5°$, with 2.5° overlap, has been applied. From the frequency distribution, determined in that way, the uniform distribution has been subtracted. The frequency distribution is contoured by isolines of 0.5 measurements per $2.5 \times 2.5°$, starting with −1.5 below (white areas) up to +3.0 (with increasingly darker gray shades) above the uniform distribution. The positions of principal crystallographic planes are indicated. The small triangle in the upper left of (A) gives a general picture of the uniform distribution, with the same contouring and gray shading as in the large triangular diagrams. The approximate deformation temperature *T* is given for each sample. (A) Sample KRGA3; measurements $n = 265$. (B) Sample KR705; $n = 385$. (C) Sample LHG4; $n = 312$. (D) Sample KR3263; $n = 386$.

patterns. This explanation forms an alternative to the model, which explains such patterns as a result of grain boundary glide along conjugate planes of high shear stress (Lister and Dornsiepen, 1982).

The presented observations and measurements provide arguments that the studied grain boundaries represent stable textures, which are at least partly controlled by temperature. The studied samples are annealed during geologically long periods well above the temperature where recrystallization and grain boundary migration of quartz start. Therefore, sufficient time and mobility should allow the grain boundaries to reach 'equilibrated' positions of whatever type. This assumption is backed by the observations on the geometry and crystallographic control of the grain boundaries as follows. (1) Independently of the different time duration as well as the temperature of annealing, the grain boundaries developed straight segments with abrupt transitions and angles from nearly 180° to well below 90° between them. (2) They form a grain boundary pattern without minimized surface but with crystallographically controlled orientations. (3) Similar temperatures resulted in similar preferred grain boundary orientations (Fig. 4B and D), despite different amounts of flow stress, strain rate and time duration. (4) Different temperatures led to different types of crystallographic preferred grain boundary orientations, with the rhombohedral $\{10\bar{1}1\}$ planes as most preferred orientations at the highest temperatures (Fig. 4A, B and D).

It may be concluded that all of the preferred crystallographic orientations of the grain boundary segments represent low-energy positions (with different energy levels) and that at increased temperatures a higher number of segments are able to reach those positions of relatively lowest energy. It is conceivable that low-index orientations, and specifically the rhombohedral planes with their strong and short bonding, form low-energy positions. In addition, the Japanese twin position is favored at low temperatures (Fig. 4A) and Estérel at higher temperatures (Fig. 4C). McLaren (1986) showed that for these twins, coincidence site lattices exist and that the twin and composition planes are commonly parallel to the plane of highest density of coincidence sites and, therefore, represent planes of relatively low energy. However, a coincidence site lattice also exists for the Breithaupt twin that does not represent a preferred grain boundary position in any of the samples. But McLaren also points to the fact that the relative grain boundary energies cannot be sufficiently predicted by the degree of matching across such a boundary or by its periodicity, and that other factors must be involved. The results of the present study are in agreement with McLaren's work because they give indications that maxima of preferred crystallographic orientations of grain boundaries partly coincide with twin positions and partly not. Many of these preferred orientations are in high-index or even crystallographically irrational positions.

But how can a straight grain boundary segment be stable in such a position? High-resolution TEM studies on gold crystals indicate that: (1) straight grain boundary segments may develop in a low-index orientation to one neighboring crystal and in a high-index or even irrational orientation to the other neighboring crystal; and (2) at these straight grain boundary segments, there is a partly ordered transition from one to the other crystal (Wolf and Merkle, 1992). Consequently, the atoms across such a boundary are bound in periodically repeated sections on the nanometer scale, whereas in other sections the crystal is strongly distorted elastically. Such a boundary may be regarded as an energetically stable structure. Even if these studies were performed only on pure tilt boundaries and, compared with rock forming minerals, on a relatively simple-structured material, the results point to a grain boundary nature that could explain the present observations on sutured quartz grain boundaries.

Finally, we would like to add some thoughts about possible principles of grain boundary development in syntectonically recrystallized quartz. In most regional and contact metamorphic rocks quartz is affected by post-deformational annealing. An exception involves continuous deformation during cooling below the recrystallization temperature of quartz. In all other cases, the deformation control of grain boundary migration, as it is included in the concept of steady-state foliation (Means, 1981) and has been demonstrated on the basis of analog material deformation (Herwegh and Handy, 1996), switches to a control of temperature and crystallography when deformation declines. The present observations suggest that the grain boundaries are stabilized as straight segments in specific crystallographically controlled low-energy positions, numerous ones at low temperatures and relatively few ones at higher temperatures. Since the development of sutured grain boundaries with straight segments is a geologically short process, as indicated by data from the present study (sample LHG4) and by other observations from pegmatites and granite intrusions in the upper crust and their contact aureoles (Warner, 1971, p. 30; Uebel, 1984, p. 88; Buntebarth and Voll, 1991), it is concluded that the crystallographically controlled stabilization of the grain boundaries is a geologically short process that takes place immediately after the termination of deformation. Consequently, the preferred crystallographic orientation of the grain boundary segments is characteristic of the temperature conditions at the termination of deformation. This suggests that grain boundaries from dynamically recrystallized quartz should generally be regarded as 'annealed' and 'equilibrated' fabrics. They are stable against subsequent annealing as long as the material is not re-deformed.

Acknowledgements

We are grateful to Jan Tullis and Christian Teyssier who not only gave numerous useful comments that improved the paper but, by their immediate response, helped us to keep abreast of the editing process. Thanks are also due to Lutz

Hecht who provided thin section material and to Klaus Haas for the preparation of the electronic figure versions.

References

Altenberger, U., Kruhl, J.H., 2000. Dry high-temperature shearing in the fossil Hercynian lower crust of Calabria (S. Italy). Periodico di Mineralogia 69, 125–142.

Buntebarth, G., Voll, G., 1991. Quartz grain coarsening by collective crystallization in contact quartzites. In: Voll, G., Töpel, J., Pattison, D.R.M., Seifert, F. (Eds.). Equilibrium and Kinetics in Contact Metamorphism. Springer, Berlin/Heidelberg, pp. 251–265.

Büttner, S., Kruhl, J.H., 1997. The evolution of a late-Variscan high-T/low-P region: the southeastern margin of the Bohemian Massif. Geologische Rundschau 86, 21–38.

von Federow, E., 1893. Nouvelle méthode pour l'étude goniométrique et optique des cristaux appliquée à la minéralogie et à la pétrographie. Mém. Comité géol. X (2), 1–191.

Gapais, D., Barbarin, B., 1986. Quartz fabric transition in a cooling syntectonic granite (Hermitage Massif, France). Tectonophysics 125, 357–370.

Gleiter, H., 1982. On the structure of grain boundaries in metals. Material Science and Engineering 52, 91–131.

Hecht, L., Vigneresse, J.L., Morteani, G., 1997. Constraints on the origin of zonation of the granite complexes in the Fichtelgebirge (Germany and Czech Republic): evidence from a gravity and geochemical study. International Journal of Earth Sciences, Supplement 86, S93–S109.

Herwegh, M., Handy, M.R., 1996. The evolution of high-temperature mylonitic microfabrics: evidence from simple shearing of a quartz analogue (norcamphor). Journal of Structural Geology 18, 689–710.

Kingery, W.D., 1974. Plausible concepts necessary and sufficient for interpretation of ceramic grain boundary phenomena: Part I. Journal American Ceramics Society 57, 1–8.

Kruhl, J.H., 1979. Deformation and metamorphism of the south-western Finero Complex (Ivrea-Zone, N. Italy) and the northerly adjacent gneiss zone. Ph.D. Thesis, University of Bonn, 131pp. (in German).

Kruhl, J.H., 2001. Crystallographic control on the development of foam textures in quartz, plagioclase and analogue material. International Journal of Earth Sciences 90, 104–117.

Kruhl, J.H., Nega, M., 1996. The fractal shape of sutured quartz grain boundaries: application as a geothermometer. Geologische Rundschau 85, 38–43.

Kunze, K., Wright, S.I., Adams, B.L., Dingley, D.J., 1993. Advances in automatic EBSP single orientation measurements. Textures and Microstructures 20, 41–54.

Lister, G.S., Dornsiepen, U.F., 1982. Fabric transitions in the Saxony granulite terrain. Journal of Structural Geology 4, 81–92.

Lloyd, G.E., 1987. Atomic number and crystallographic contrast images with the SEM: a review of backscattered electron techniques. Mineralogical Magazine 51, 3–19.

Masberg, H.P., Hoffer, E., Hoernes, S., 1992. Microfabrics indicating granulite-facies metamorphism in the low-pressure central Damara Orogen, Namibia. Precambrian Research 55, 243–257.

McLaren, A.C., 1986. Some speculations on the nature of high-angle grain boundaries in quartz rocks. In: Hobbs, B.E., Heard, H.C. (Eds.). Mineral and Rock Deformation: Laboratory Studies — The Paterson Volume. American Geophysical Union, Washington, DC., Geophysical Monograph 36, pp. 233–245.

Means, W.D., 1981. The concept of steady-state foliation. Tectonophysics 78, 179–199.

Norton, M.G., Carter, C.B., 1992. Grain and interphase boundaries in ceramics and ceramic composites. In: Wolf, D., Yip, S. (Eds.). Materials Interfaces. Chapman & Hall, London, pp. 151–189.

Passchier, C.W., Trouw, R.A.J., 1996. Microtectonics. Springer, Berlin/Heidelberg/New York.

Poirier, J.-P., Guillopé, M., 1979. Deformation-induced recrystallization of minerals. Bulletin Mineralogie 102, 67–74.

Prior, D.J., Trimby, P.W., Weber, U., 1996. Orientation contrast imaging of microstructures in rocks using forescattered detectors in the scanning microscope. Mineralogical Magazine 60, 859–869.

Sarantschina, G.M., 1963. Die Fedorow-Methode. VEB Deutscher Verlag der Wissenschaften, Berlin.

Schenk, V., 1989. P–T–t path of the lower crust in the Hercynian fold belt of southern Calabria. In: Daley, J.S., Cliff, R.A., Yardley, B.W.D. (Eds.). Evolution of Metamorphic Belts. Geological Society Special Publication 43, pp. 337–342.

Siebel, W., Trzebski, R., Stettner, G., Hecht, L., Casten, U., Höhndorf, A., Müller, P., 1997. Granitoid magmatism of the NW Bohemian massif revealed: gravity data, composition, age relations and phase concept. Geologische Rundschau 86, S45–S63.

Trümpy, R., 1980. Geology of Switzerland. Part A. Wepf & Co, Basel/New York.

Uebel, R., 1984. Graphic granites: their problems and petrogenesis. Ph.D. Thesis, Technical University Berlin, D83 (in German).

Vernon, R.H., 1976. Metamorphic Processes. Allen & Unwin, London.

Voll, G., 1969. Klastische Mineralien aus den Sedimentserien der Schottischen Highlands und ihr Schicksal bei aufsteigender Regional- und Kontaktmetamorphose. Habilitationsschrift, Fakultät für Bergbau und Hüttenwesen, Technische Universität Berlin, D83.

Voll, G., 1976. Recrystallization of quartz, biotite and feldspars from Erstfeld to the Leventina Nappe, Swiss Alps, and its geological significance. Schweizerische mineralogische und petrographische Mitteilungen 56, 641–647.

Wagner, G.A., Reimer, G.M., Jäger, E., 1977. Cooling ages derived by apatite fission-track, mica Rb–Sr and K–Ar dating: the uplift and cooling history of the Central Alps. Memorie degli Istituti di Geologia e Mineralogia dell'Università di Padova, Vol. XXX, 1–27.

Warner, E.M., 1971. Petrology and structural geology of igneous and metamorphic rocks, west side of Eureka Valley, Inyo Mountains, California. M.Sc. Thesis, University of California, Los Angeles.

Wolf, D., Merkle, K.L., 1992. Correlation between the structure and energy of grain boundaries in metals. In: Wolf, D., Yip, S. (Eds.). Materials Interfaces. Chapman & Hall, London, pp. 87–150.